Food Chemistry 444 (2024) 138516

Contents lists available at ScienceDirect

Food Chemistry

journal homepage: www.elsevier.com/locate/foodchem

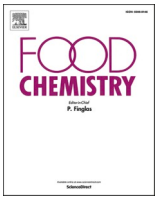

Effect of olive leaf phytochemicals on the anti-acetylcholinesterase, anti-cyclooxygenase-2 and ferric reducing antioxidant capacity

Jose M. Romero-Márquez [a,1], María D. Navarro-Hortal [a,1], Tamara Y. Forbes-Hernández [a,*], Alfonso Varela-López [a], Juan G. Puentes [b], Cristina Sánchez-González [a,c], Sandra Sumalla-Cano [d], Maurizio Battino [d,e,f,g], Roberto García-Ruiz [b], Sebastián Sánchez [b], José L. Quiles [a,d,*]

[a] Department of Physiology, Institute of Nutrition and Food Technology "José Mataix Verdú", Biomedical Research Centre, University of Granada, 18016 Armilla, Spain
[b] University Institute of Research in Olive Grove and Olive Oils, University of Jaén, 23071 Jaén, Spain
[c] Sport and Health Research Centre, University of Granada, C/Menéndez Pelayo 32, 18016 Granada, Spain
[d] Research Group on Foods, Nutritional Biochemistry and Health, Universidad Europea del Atlántico, Isabel Torres, 21, 39011 Santander, Spain
[e] Department of Health, Nutrition and Sport, Iberoamerican International University, Campeche, 24560, Mexico
[f] Department of Clinical Sciences, Polytechnic University of Marche, 60131 Ancona, Italy
[g] International Joint Research Laboratory of Intelligent Agriculture and Agri-products Processing, Jiangsu University, Zhenjiang 212013, China

ARTICLE INFO

Keywords:
Cholinergic
AChE
COX
Inflammation
Iron
Oxidative stress
Olive
Leaves

ABSTRACT

In this study, the phytochemical profile of fifty olive leaves (OL) extracts from Spain, Italy, Greece, Portugal, and Morocco was characterized and their anti-cholinergic, anti-inflammatory, and antioxidant activities were evaluated. Luteolin-7-*O*-glucoside, isoharmnentin, and apigenin were involved in the acetylcholinesterase (AChE) inhibitory activity, while oleuropein and hydroxytyrosol showed noteworthy potential. Secoiridoids contributed to the cyclooxygenase-2 inhibitory activity and antioxidant capacity. Compounds such as oleuropein, ligstroside and luteolin-7-*O*-glucoside, may exert an important role in the ferric reducing antioxidant capacity. It should be also highlighted the role of hydroxytyrosol, hydroxycoumarins, and verbascoside concerning the antioxidant activity. This research provides valuable insights and confirms that specific compounds within OL extracts contribute to distinct anti-cholinergic, anti-inflammatory, and anti-oxidative effects.

1. Introduction

Olive leaves (OL), the verdant appendages of the *Olea europaea* tree, exhibit distinctive morphology characterized by lanceolate shapes and a silver-green color palette, contributing to the overall aesthetic appeal of olive groves (Blazakis et al., 2017). In the lifecycle of olive cultivation, these leaves become integral components, yet their eventual disposal results in the generation of agricultural waste in the form of pruning and fallen foliage. These by-products significantly contribute to the environmental footprint of olive oil production, owing to the substantial water and energy resources required for their disposal, along with the associated gas emissions and waste generation. On a global scale, the European Union (EU) stands as the foremost producer of olive by-products, with Spain, Greece, Italy, and Portugal collectively accounting for nearly 99 % of the EU's production (Espeso et al., 2021). Although olive leaves are predominantly utilized for purposes such as animal consumption, biomass production, or incineration, their comprehensive utilization and sustainable management remain critical considerations in addressing the environmental impact of the olive grove industry (C. Zhang et al., 2022). OL are rich reservoirs of diverse bioactive compounds, including secoiridoids like oleuropein, phenolic alcohols such as hydroxytyrosol, flavonoids like luteolin and luteolin-7-*O*-glucoside, and phenolic acids like verbascoside (Romero-Márquez, Forbes-Hernández, et al., 2023). These compounds present potential applications beyond traditional uses, particularly in the development of nutraceuticals (Romero-Márquez, Navarro-Hortal, Jiménez-Trigo, Vera-

Abbreviations: Ach, acetylcholine; AChE, acetylcholinesterase; A-DM elenolic acid, aldehydic form of decarboxymethyl elenolic acid; ANOVA, analysis of variance; COX-2, cyclooxygenase-2; FRAP, ferric reducing antioxidant power; Min, minutes; OL, olive leaves; PLS-DA, Partial least squares-discriminant analysis; SD, standard deviation; SEM, standard error of the mean; VIP, variable of importance in projection.

* Corresponding authors.
E-mail addresses: tforbes@ugr.es (T.Y. Forbes-Hernández), jlquiles@ugr.es (J.L. Quiles).
[1] These authors contributed equally to this work.

https://doi.org/10.1016/j.foodchem.2024.138516
Received 8 November 2023; Received in revised form 16 January 2024; Accepted 18 January 2024
Available online 23 January 2024

Ramírez, et al., 2022). Olive leaves have exhibited noteworthy biomedical properties, including antiviral, antimicrobial, anti-inflammatory, antioxidant, and anti-cholinergic activities (Alcántara et al., 2020; Lama-Muñoz et al., 2020; Romero-Márquez et al., 2021; Romero-Márquez, Forbes-Hernández, et al., 2023).

Recently, the connection between the profile and content of phytochemicals in OL extracts and their antioxidant capacity has been established (C. Zhang et al., 2022). Consequently, the applications of OL may be influenced by the composition and concentration of these compounds. These considerations highlight the multifaceted nature of OL phytochemistry, emphasizing the need for a comprehensive understanding of the role of phytochemical content and, consequently, the functional properties of OL extracts. Certain *in vitro* assessments, including the evaluation of acetylcholinesterase (AChE) and cyclooxygenase (COX)-2 inhibitory capacities, as well as ferric reducing antioxidant potential (FRAP) enable a comprehensive examination of the neuroprotective, anti-inflammatory and antioxidants effects of specific compounds of interest. Hence, the hypothesis of this work postulates that certain compounds present in OL extracts contribute to their anti-cholinergic, anti-inflammatory, and anti-oxidative effects. To investigate this, a thorough phytochemical characterization of fifty OL extracts was carried out, focusing on their anti-AChE, anti-COX-2 and FRAP. Furthermore, an in-depth examination of the individual contributions of each compound was conducted, aiming to enhance our understanding of their respective impacts on the observed effects.

2. Material and methods

2.1. Chemicals and reagents

Analytical grade reagents and chemicals were purchased from Sigma-Aldrich (Missouri, USA), Thermo Fisher (Massachusetts, USA), Merck (Darmstadt, Germany) or Roche (Basel, Switzerland) and the water used was Milli-Q type (resistivity 18.2 MΩcm) obtained from Millipore purification equipment (Massachusetts, USA).

2.2. Olive leaves obtaining, classification, and extraction

A total of 49 OL samples were obtained from Spain, Italy, Greece, Portugal as previously described (Romero-Márquez, Navarro-Hortal, et al., 2023). Plus, one additional OL sample was obtained from Ouezzan, Morocco and provided by Alhouda cooperative. The OL used were those collected along with the olives during the harvesting procedure in the olive mill, discarding leaves from the ground or collected directly from the tree. For the extraction, the 50 OL samples were dried, ground, and passed through a mesh sieve to obtain a fine powder. Then, the dried OL powder was mixed with extraction buffer (ethanol/Mili-Q water/formic acid, 80:20:0.1, v:v:v) and mixed for two hours at room temperature in the dark. Then, OL mixture was centrifuged, and the supernatant was recovered and filtered using a 0.45 μm syringe filter (PBI International, Italy). Finally, the samples were aliquoted, evaporated using an Speedvac SC110A (New York, USA), and stored at –80 °C until analyses (Rivas-García et al., 2021).

2.3. Identification and quantification of the phytochemical compounds via HPLC-ESI-QTOF-MS/MS analysis

HPLC analyses were performed on an Agilent 1260 HPLC instrument (California, USA) equipped with a binary pump, an online degasser, an auto-sampler, a thermostatically controlled column compartment, as well as a diode array detector (Romero-Márquez, Navarro-Hortal, et al., 2023). The samples were separated on an Agilent Zorbax Eclipse Plus C18 column (1.8 μm, 4.6 × 150 mm). The mobile phases consisted of water with 0.1 % formic acid (A) and methanol with 0.1 % formic acid (B) using a gradient elution according to the following profile: 0 min (min), 5 % B; 5 min, 75 % B; 10 min, 100 % B; 18 min, 100 % B; 25 min, 5 % B. The initial conditions were maintained for 5 min. The flow rate was 0.8 mL/min, the column temperature, 30 °C, and the injection volume, 5 μL.

Detection was performed using an Agilent 6540 Ultra High Definition (UHD) Accurate-Mass Q-TOF mass spectrometer in negative ion mode within a mass range of 50–1700 *m/z*. The operating parameters were as follows: drying gas flow rate, 10 L/min; drying gas temperature, 325 °C; nebulizer, 60 psi; sheath gas temperature, 400 °C; sheath gas flow, 12 L/min; capillary, 4000 V; fragmentor, 130 V. The MS/MS analyses were acquired by automatic fragmentation where the two most intense mass peaks were fragmented with the following collision energy values: 10, 20, 30 and 40 eV. Continuous infusion of the reference ions *m/z* 112.985587 (trifluoroacetate anion) and 1033.988109 (adduct of hexakis (1H,1H, 3H-tetrafluoropropoxy) phosphazine or HP-921) was used to correct each mass spectrum. All the operations, acquisition and analysis of data were controlled by Masshunter workstation software version B.06.00 (Agilent Technologies, USA).

The 50 samples were resuspended in ethanol/water (50:50, v:v) at a concentration of 10 mg/mL and filtered through a 0.20 μm PTFE syringe filter before injection into the chromatographic system. The main compounds in the sample were detected automatically using a compound extraction algorithm based on the detection of molecular characteristics, and the resulting peaks were filtered with a relative volume threshold of 0.2 % as well as those appearing in the solvent blank. Additionally, characteristic compounds of olive leaves were searched in a targeted way. The compounds detected by this algorithm were tentatively identified whenever possible with the help of compound databases and scientific literature related to *Olea europaea*, based on the molecular formula obtained from the exact mass and isotopic distribution data, at the retention times and fragmentation patterns recorded.

For quantification, the compound concentrations of each OL extract were determined by using the area under the peak and by interpolation in the corresponding calibration curve. The HPLC analytical grade (>90 % purity) standards used were: oleuropein (secoridoids), luteolin and luteolin-7-*O*-glucoside (flavonoids), hydroxytyrosol (phenolic alcohols and acids), loganin (iridoids), 6-hydroxycoumarin (hydroxycoumarins), and verbascoside (hydroxycinnamic acid). Oleuropein and hydroxytyrosol were also used for lauroside B and azelaic acid quantification, respectively, which were included in other compounds section. Oleuropein, hydroxytyrosol, luteolin, luteolin-7-*O*-glucoside, verbascoside, loganin, and 6-hydroxycoumarin were quantified by the calibration curves obtained from their respective commercial standards. The remaining compounds were semi-quantified based on calibration curves from other compounds with structural similarities (Figure S1, Table S1, and Table S2). Results are expressed as mean ± standard deviation (SD).

2.4. AChE inhibition assay

The colorimetric method proposed by Ellman was applied to determine the AChE inhibitory activity of OL extracts (Ellman et al., 1961). Briefly, OL extracts (1000 μg/mL) were incubated with AChE (10 mU/mL) and 5,5′-dithiobis-(2-nitrobenzoic acid) (150 μM) in a 96-plate wells for 15 min at 30 °C. Then, the acetylthiocholine iodide was added, and the AChE activity was determined recording the changes in the absorbance at 405 nm in a Synergy 2 Biotek plate reader (Vermont, USA) for 25 min at 30 °C. The AChE inhibitory activities were expressed as the mean percentage of inhibitory activity with respect to the positive control ± standard error of the mean (SEM).

2.5. COX-2 inhibition assay

COX-2 inhibitory activity was measured using a Biovision COX-2 Inhibitor Screening Kit (California, USA) following the commercial protocol (Romero-Márquez, Navarro-Hortal, et al., 2023). Briefly, OL extracts (1 μg/mL, in the reaction mixture) were incubated with a solution containing arachidonic acid and sodium hydroxide as well as the

reaction mix in a black 96-plate wells for at 37 °C. The fluorescent signal was recorded at 535 and 587 nm for extinction and emission, respectively, in Synergy 2 Biotek plate reader (Vermont, USA) for 8 min. The COX-2 inhibitory activities were expressed as the mean percentage of inhibitory activity with respect to the positive control ± SEM.

2.6. Ferric reducing antioxidant power

The FRAP method was performed following the modified protocol described by Rivas-García *et al.* (Rivas-García et al., 2022). FRAP is an electronic transfer-based method, which analyzes the ability of a specific antioxidant to reduce the complex formed by ferric iron and 2,4,6-tripyridyl-s-triazine, changing the color during this reaction. The magnitude of the color change is directly associated with the antioxidant concentration in the sample. The units were expressed as the mean of μM of Trolox per gram of dry weight of extract ± SEM.

2.7. Statistical analysis

The experimental procedures were performed at least three times. The statistical software IBM SPSS 25 (Illinois, USA) was used for the analysis of normality, variance homogeneity, analysis of variance (ANOVA) and Pearson's correlation analysis. ANOVA was conducted, and *post hoc* Duncan's Multiple Range test was employed under the assumptions of normality and variance homogeneity. In cases where homogeneity of variances was not assumed, the *post hoc* Games-Howell test was applied. All tests were considered statistically significant at a threshold of $p < 0.05$. Partial least squares-discriminant analysis (PLS-DA) was applied using MetaboAnalyst V5.0 software. PLS-DA was used to analyze the normalized and auto-scaled mean values of the 42 compounds from 50 OL extracts analyzed by HPLC-ESI-QTOF-MS/MS and its relationship with cholinesterase, inflammatory, and iron-oxidative inhibitory activity. In the present PLS-DA, the selection criteria of the variable of importance in projection (VIP) score was values higher than 1, which correspond to $p < 0.05$.

3. Results and discussion

3.1. Phytochemical profile of olive leaf extracts based on the AChE inhibitory activity

As far as it's known, this is the first study describing the optimal phytochemical composition of OL for AChE inhibition on a large-scale *in vitro*. For this purpose, the 50 OL extracts were divided into four subpopulations based on the activity of the different OL extracts to inhibit AChE (Table S3) into high (A1, n = 13), medium–high (A2, n = 12), medium–low (A3, n = 12), and low (A4, n = 13) subpopulations (Figure S2) determined by quartile distribution. Then, the 42 compounds reported from each OL extract, which included 16 flavonoids, 14 secoiridoids, 3 phenolic alcohols, 3 iridoids, 2 hydroxycoumarins, 2 hydroxycinnamic acids, and 1 phenolic acid and other compound were clustered in each subpopulation. After that, the mean for each compound was calculated and was used as representative value of each subpopulation concerning AChE inhibitory activity.

Table 1 shows the phytochemical profile of these subpopulations, obtained from the individual characterization of all the OL extracts that compose each of them. The content of secoiridoids seems to influence the modulatory activity of the AChE inhibitors exhibited by OL since more than 70 % of the studied secoiridoids were different between A1 and A4 subpopulations. In this context, the OL extracts from A1 presented higher content in oleuropein and its derivatives (oleuropein diglucoside, oleuropein isomer, and hydroxyoleuropein), oleoside methyl ester, and ligstroside content compared to OL extracts from A4 subgroup. In fact, oleuropein and its derivatives (oleuropein diglucoside, oleuropein isomer) as well as ligstroside content were different between A1 and A2 subpopulations, indicating that these secoiridoids

Table 1
Phytochemical profile (milligram of compound per gram of dry weight) of the OL extracts based on AChE inhibitory activity.

	A4	A3	A2	A1
Secoiridoids				
1-β-D-Glu-ACD EA I1	0.29 ± 0.26	0.30 ± 0.15	0.39 ± 0.19	0.26 ± 0.18
1-β-D-Glu-ACD EA I2	0.51 ± 0.70	0.78 ± 0.62	0.79 ± 0.54	0.49 ± 0.30
A-DM EA	0.34 ± 0.46^{b}	0.13 ± 0.13^{ab}	0.18 ± 0.18^{ab}	0.07 ± 0.11^{a}
D-OH EA I2	0.08 ± 0.19	–	–	–
H-DA-DM EA	0.11 ± 0.18^{b}	0.03 ± 0.04^{ab}	0.03 ± 0.05^{ab}	0.01 ± 0.03^{a}
Hy-DA-DM EA I1	0.07 ± 0.12	0.13 ± 0.09	0.13 ± 0.11	0.09 ± 0.14
Hy-DA-DM EA I2	0.43 ± 0.54^{b}	0.16 ± 0.25^{ab}	0.14 ± 0.16^{ab}	0.05 ± 0.15^{a}
Hydroxyoleuropein	0.04 ± 0.10^{a}	0.19 ± 0.38^{ab}	0.17 ± 0.28^{ab}	0.53 ± 0.698^{b}
Ligstroside	–	0.06 ± 0.20^{a}	0.07 ± 0.24^{a}	0.32 ± 0.44^{b}
Oleoside	0.47 ± 0.97	0.91 ± 1.38	0.65 ± 1.90	1.92 ± 2.59
Oleoside methyl ester	0.23 ± 0.37^{a}	0.75 ± 0.81^{ab}	0.71 ± 1.71^{ab}	1.40 ± 1.60^{b}
Oleuropein	1.04 ± 2.19^{a}	3.29 ± 9.25^{a}	3.76 ± 10.9^{a}	15.00 ± 22.00^{b}
Oleuropein diglu	–	0.02 ± 0.06^{a}	0.02 ± 0.08^{a}	0.19 ± 0.30^{b}
Oleuropein I	0.06 ± 0.19^{a}	0.27 ± 0.92^{a}	0.35 ± 1.21^{a}	1.50 ± 2.22^{b}
Flavonoids				
(+)-Eriodictyol	0.05 ± 0.08	0.13 ± 0.12	0.11 ± 0.13	0.04 ± 0.09
Apigenin	0.19 ± 0.15	0.17 ± 0.14	0.24 ± 0.32	0.12 ± 0.25
Apigenin-7-*O*-glu	0.20 ± 0.21	0.31 ± 0.14	0.28 ± 0.19	0.33 ± 0.27
Apigenin-7-*O*-rut	0.27 ± 0.16	0.44 ± 0.20	0.45 ± 0.26	0.45 ± 0.23
Chrysoeriol-7-*O*-glu	0.36 ± 0.29^{a}	0.58 ± 0.20^{ab}	0.54 ± 0.21^{ab}	0.70 ± 0.17^{b}
Diosmetin	0.26 ± 0.17	0.19 ± 0.09	0.25 ± 0.16	0.20 ± 0.20
I-3-*O*-β-D-glu	0.01 ± 0.03	0.01 ± 0.02	0.02 ± 0.02	0.07 ± 0.08
Luteolin	0.24 ± 0.17	0.22 ± 0.14	0.33 ± 0.23	0.37 ± 0.23
Luteolin 7-*O*-glu	0.47 ± 0.35^{a}	0.88 ± 0.49^{a}	0.96 ± 0.39^{a}	2.00 ± 1.76^{b}
Luteolin glu	2.21 ± 1.74^{a}	4.12 ± 2.04^{ab}	3.94 ± 2.24^{b}	5.01 ± 1.98^{b}
Luteolin rut I1	–	–	0.01 ± 0.00	0.00 ± 0.01
Luteolin rut I2	0.01 ± 0.01	0.01 ± 0.02	0.02 ± 0.04	0.04 ± 0.06
Luteolin-7,4-*O*-diglu	0.03 ± 0.05^{a}	0.09 ± 0.07^{a}	0.09 ± 0.08^{b}	0.13 ± 0.07^{b}
Oxidized quercetin	–	–	–	0.01 ± 0.01
Taxifolin	0.01 ± 0.01	–	0.01 ± 0.01	0.01 ± 0.02
Phenolic alcohols				
Hydroxytyrosol	0.08 ± 0.07^{a}	0.11 ± 0.11^{ab}	0.13 ± 0.09^{ab}	0.20 ± 0.19^{b}
Hydroxytyrosol glu	0.15 ± 0.18^{a}	0.18 ± 0.14^{a}	0.41 ± 0.58^{ab}	0.68 ± 0.73^{b}
4-Ethylguaiacol	0.4 ± 0.11^{b}	0.09 ± 0.02^{ab}	0.08 ± 0.02^{ab}	0.06 ± 0.06^{a}
Iridoids				
Loganic acid	0.16 ± 0.11	0.23 ± 0.09	0.22 ± 0.09	0.28 ± 0.08
7-Epiloganin	0.57 ± 0.35	0.64 ± 0.26	0.75 ± 0.29	0.71 ± 0.27
Lamiol	0.61 ± 0.46	0.82 ± 0.32	0.91 ± 0.54	0.79 ± 0.48

(*continued on next page*)

Table 1 (*continued*)

	A4	A3	A2	A1
Hydroxycoumarins				
Esculetin	0.13 ± 0.20	0.18 ± 0.20	0.19 ± 0.16	0.22 ± 0.26
Esculin	0.04 ± 0.05	0.06 ± 0.04	0.06 ± 0.04	0.06 ± 0.06
Hydroxycinnamic acid				
Verbascoside	0.15 ± 0.12[a]	0.27 ± 0.40[ab]	0.28 ± 0.34[ab]	0.51 ± 0.58[b]
Decaffeoylverbascoside	0.80 ± 0.88[a]	0.99 ± 0.42[ab]	1.24 ± 0.86[ab]	1.63 ± 0.94[b]
Phenolic acids				
p-Hydroxybenzoic acid	0.02 ± 0.02	0.03 ± 0.01	0.03 ± 0.01	0.06 ± 0.11
Other compounds				
Lauroside B	0.37 ± 0.52	0.31 ± 0.25	0.30 ± 0.24	0.39 ± 0.25
Azelaic acid	0.34 ± 0.32	0.65 ± 0.78	0.89 ± 1.23	0.46 ± 0.49

might contribute substantially to the AChE inhibitory activity.

Results are expressed as mean ± SD. For each parameter, columns with different letters indicate statistically significant differences between subpopulations ($p < 0.05$). Abbreviations: 1-β-D-Glu-ACD elenolic acid I1: 1-β-D-Glucopyranosyl acyclodihydroelenolic acid isomer 1; 1-β-D-Glu-ACD elenolic acid I2: 1-β-D-Glucopyranosyl acyclodihydroelenolic acid isomer 2; A-DM elenolic acid: aldehydic form of decarboxymethyl elenolic acid; D-OH elenolic acid I2: decarboxylated form of hydroxy elenolic acid isomer 2; EA: elenolic acid; glu: glucoside; H-DA-DM elenolic acid: hydrated product of the dialdehydic form of decarboxymethyl elenolic acid; Hy-DA-DM elenolic acid I1: hydroxylated product of the dialdehydic form of decarboxymethyl elenolic acid isomer 1; Hy-DA-DM elenolic acid I2: hydroxylated product of the dialdehydic form of decarboxymethyl elenolic acid isomer 2; *m/z*: mass to charge ratio; OL: olive leaves; I: isomer; rut: rutinoside.

A substantial difference was also found for the flavonoid contents between A1 and A4 subpopulations. Specifically, OL extracts from A1 presented higher content in luteolin derivatives (luteolin 7-*O*-glucoside, luteolin-7,4-*O*-diglucoside, luteolin glucoside, and luteolin rutinoside isomer 1 and 2), chrysoeriol-7-*O*-glucoside, and isorhamnetin 3-*O*-β-D-(6-p-coumaroyl) glucoside compared with those OL from A4 subpopulation. Among flavonoids, the content in luteolin-7-*O*-glucoside and isorhamnetin 3-*O*-β-D-(6-p-coumaroyl) glucoside might also contribute to the AChE inhibitory activity since their content was two and three times, respectively higher than the observed in A2 subpopulation. On the other hand, the phenolic alcohol (hydroxytyrosol and hydroxytyrosol glucoside), hydroxycinnamic acid (verbascoside and decaffeoylverbascoside), and iridoid (loganic acid) content were higher in OL from the A1 compared with those from A4 but not with A2 subpopulations. Surprisingly, and in contrast to the aforementioned results, over 25 % of the examined secoiridoids corresponded to elenolic acid derivatives, which were found to be more abundant in the OL extracts from A4 subpopulations. A similar pattern was observed with phenolic alcohols such as 4-Ethylguaiacol in A4 subpopulations, indicating a possible negative relation between these compounds and the AChE inhibitory activity.

3.2. Phytochemical profile of olive leaf extracts based on the COX-2 inhibitory activity

As mentioned with AChE inhibitory activity, this is the first study describing the optimal phytochemical composition of OL for COX-2 inhibition on a large-scale *in vitro*. For this purpose, the 50 OL extracts were divided into four subpopulations based on the activity of the different OL extracts to inhibit COX-2 (Table S3) into high (C1, n = 13), medium–high (*C*2, n = 12), medium–low (C3, n = 12), and low (C4, n = 13) subpopulations (Figure S3) determined by quartile distribution. Then, the 42 compounds previously reported in OL by HPLC-QTOF MS analysis, were clustered in each subpopulation. After that, the mean for each compound was calculated and was used as representative value of each subpopulation concerning COX-2 inhibitory activity (Table 2).

The content of secoiridoids seems to influence the modulatory activity of the COX-2 exhibited by OL since over 55 % of the studied secoiridoids were different between C1 and C4 subpopulations. In this context, the OL extracts from C1 presented higher content in oleuropein and its derivatives (oleuropein diglucoside, oleuropein isomer, and hydroxyoleuropein), oleoside and its derivatives (oleoside methyl ester), and ligstroside in comparison with those OL extracts from C4 subgroup. Oleuropein derivatives (oleuropein diglucoside and hydroxyoleuropein), oleoside and its derivatives as well as ligstroside contents seem to exhibit an important anti-inflammatory role since C1 and *C*2 subpopulations were different in these compounds. Similarly, C1 and C3 subpopulations were different in these secoiridoids, indicating that these compounds might contribute to COX-2 inhibitory activity.

Results are expressed as mean ± SD. For each parameter, columns with different letters indicate statistically significant differences between subpopulations ($p < 0.05$). Abbreviations: 1-β-D-Glu-ACD elenolic acid I1: 1-β-D-Glucopyranosyl acyclodihydroelenolic acid isomer 1; 1-β-D-Glu-ACD elenolic acid I2: 1-β-D-Glucopyranosyl acyclodihydroelenolic acid isomer 2; A-DM elenolic acid: aldehydic form of decarboxymethyl elenolic acid; D-OH elenolic acid I2: decarboxylated form of hydroxy elenolic acid isomer 2; EA: elenolic acid; glu: glucoside; H-DA-DM elenolic acid: hydrated product of the dialdehydic form of decarboxymethyl elenolic acid; Hy-DA-DM elenolic acid I1: hydroxylated product of the dialdehydic form of decarboxymethyl elenolic acid isomer 1; Hy-DA-DM elenolic acid I2: hydroxylated product of the dialdehydic form of decarboxymethyl elenolic acid isomer 2; *m/z*: mass to charge ratio; OL: olive leaves; I: isomer; rut: rutinoside.

COX-2 modulatory activity seems to be less influenced by flavonoid content in comparison with AChE inhibitory activity. In this case, only the 19 % of the flavonoids studied were statistically different between C1 and C4 subpopulations, while about 50 % of the flavonoids studied were different in A1 and A4 subpopulations (AChE inhibitory activity subgroups). In this context, OL extracts from C1 showed the highest content in luteolin 7-*O*-glucoside over the rest, indicating a possible modulatory effect of this compound on neuroinflammation. Similarly, the isorhamnetin 3-*O*-β-D-(6-p-coumaroyl) glucoside content was also higher, but only compared with those OL extracts from C4 subgroup. Likewise, as luteolin-7-*O*-glucoside, the verbascoside content was also distinguished on C1 over the rest. In contrast to the results, but in the same line with the results obtained in the previous section, the content of elenolic acid derivatives such as hydroxylated product of the dialdehydic form of decarboxymethyl elenolic acid isomer 1 as well as the flavonoid diosmetin were more abundant in the OL extracts from C4 subpopulations, indicating a possible negative relation between these compounds and the COX-2 inhibitory activity.

3.3. Phytochemical profile of olive leaf extracts based on FRAP

The 50 OL extracts were divided into four subpopulations concerning their ferric reducing antioxidant power activity (Table S3) into high (F1, n = 13), medium–high (F2, n = 12), medium–low (F3, n = 12), and low (F4, n = 13) subpopulations (Figure S4) determined by quartile distribution. Then, the 42 compounds previously reported in OL by HPLC-QTOF MS analysis, were clustered in each subpopulation. After that, the mean for each compound was calculated and was used as representative value of each subpopulation concerning FRAP (Table 3).

The content of secoiridoids seems to strongly influence the ferric reducing antioxidant power exhibited by OL since the 50 % of the studied secoiridoids were more abundant in the OL extracts from F1 subpopulation. Specifically, the OL extracts from F1 had the highest content in oleuropein and its derivatives, oleoside and its derivatives,

Table 2
Phytochemical profile (milligram of compound per gram of dry weight) of the OL extracts based on COX-2 inhibitory activity.

	C4	C3	C2	C1
Secoiridoids				
1-β-D-Glu-ACD EA I1	0.34 ± 0.19	0.29 ± 0.16	0.33 ± 0.25	0.27 ± 0.22
1-β-D-Glu-ACD EA I2	0.56 ± 0.55	0.79 ± 0.60	0.50 ± 0.52	0.70 ± 0.58
A-DM EA	0.09 ± 0.13^{a}	0.15 ± 0.21^{ab}	0.33 ± 0.44^{b}	0.16 ± 0.21^{ab}
D-OH EA I2	–	–	0.08 ± 0.20	–
H-DA-DM EA	0.02 ± 0.05	0.05 ± 0.10	0.06 ± 0.13	0.04 ± 0.12
Hy-DA-DM EA I1	0.16 ± 0.14^{b}	0.08 ± 0.10^{ab}	0.11 ± 0.13^{a}	0.06 ± 0.08^{a}
Hy-DA-DM EA I2	0.14 ± 0.26^{ab}	0.20 ± 0.19^{ab}	0.39 ± 0.58^{b}	0.08 ± 0.13^{a}
Hydroxyoleuropein	0.03 ± 0.06^{a}	0.06 ± 0.10^{a}	0.21 ± 0.29^{a}	0.62 ± 0.70^{b}
Ligstroside	–	–	0.08 ± 0.28^{a}	0.36 ± 0.42^{b}
Oleoside	0.14 ± 0.15^{a}	0.45 ± 0.95^{a}	0.68 ± 1.80^{ab}	2.65 ± 2.46^{b}
Oleoside methyl ester	0.29 ± 0.31^{a}	0.36 ± 0.71^{a}	0.52 ± 0.94^{a}	1.88 ± 1.88^{b}
Oleuropein	0.57 ± 0.56^{a}	0.98 ± 2.23^{a}	6.47 ± 19.70^{ab}	15.00 ± 17.30^{b}
Oleuropein diglu	–	–	0.04 ± 0.14^{a}	0.19 ± 0.28^{b}
Oleuropein I	0.01 ± 0.01^{a}	0.06 ± 0.20^{a}	0.57 ± 1.97^{ab}	1.55 ± 1.79^{b}
Flavonoids				
(+)-Eriodictyol	0.09 ± 0.12	0.04 ± 0.06	0.12 ± 0.14	0.07 ± 0.09
Apigenin	0.23 ± 0.23	0.19 ± 0.22	0.23 ± 0.30	0.07 ± 0.07
Apigenin-7-*O*-glu	0.29 ± 0.14	0.20 ± 0.18	0.29 ± 0.23	0.328 ± 0.27
Apigenin-7-*O*-rut	0.46 ± 0.19	0.35 ± 0.27	0.46 ± 0.22	0.33 ± 0.19
Chrysoeriol-7-*O*-glu	0.63 ± 0.11	0.49 ± 0.28	0.49 ± 0.28	0.56 ± 0.29
Diosmetin	0.30 ± 0.14^{b}	0.24 ± 0.15^{b}	0.25 ± 0.19^{b}	0.12 ± 0.11^{a}
I-3-*O*-β-D-glu	0.01 ± 0.01	0.02 ± 0.03	0.03 ± 0.03	0.05 ± 0.09
Luteolin	0.30 ± 0.20	0.33 ± 0.21	0.31 ± 0.23	0.23 ± 0.19
Luteolin 7-*O*-glu	0.68 ± 0.19^{a}	0.75 ± 0.37^{a}	0.95 ± 0.53^{ab}	1.93 ± 1.86^{b}
Luteolin glu	4.08 ± 1.56	3.55 ± 2.61	3.91 ± 2.58	3.69 ± 2.21
Luteolin rut I1	0.01 ± 0.01	–	0.01 ± 0.01	–
Luteolin rut I2	0.01 ± 0.04	0.02 ± 0.04	0.02 ± 0.04	0.03 ± 0.05
Luteolin-7,4-*O*-diglu	0.09 ± 0.06	0.08 ± 0.09	0.10 ± 0.10	0.07 ± 0.07
Oxidized quercetin	–	–	0.01 ± 0.01	–
Taxifolin	–	–	0.01 ± 0.02	0.01 ± 0.01
Phenolic alcohols				
Hydroxytyrosol	0.10 ± 0.08	0.13 ± 0.11	0.10 ± 0.10	0.19 ± 0.19
Hydroxytyrosol glu	0.21 ± 0.30	0.42 ± 0.58	0.23 ± 0.31	0.56 ± 0.71
4-Ethylguaiacol	0.06 ± 0.04	0.10 ± 0.05	0.11 ± 0.10	0.10 ± 0.07
Iridoids				
Loganic acid	0.22 ± 0.10	0.21 ± 0.12	0.19 ± 0.08	0.27 ± 0.11
7-Epiloganin	0.67 ± 0.26	0.64 ± 0.31	0.74 ± 0.38	0.62 ± 0.25
Lamiol	0.78 ± 0.50	0.68 ± 0.52	0.78 ± 0.46	0.88 ± 0.39
Hydroxycoumarins				
Esculetin	0.19 ± 0.22	0.19 ± 0.22	0.15 ± 0.16	0.18 ± 0.23
Esculin	0.04 ± 0.03	0.04 ± 0.03	0.05 ± 0.06	0.08 ± 0.06
Hydroxycinnamic acid				
Verbascoside	0.13 ± 0.06^{a}	0.21 ± 0.16^{a}	0.22 ± 0.37^{a}	0.65 ± 0.59^{b}
Decaffeoylverbascoside	1.37 ± 0.92	1.17 ± 0.98	1.16 ± 0.90	0.96 ± 0.60
Phenolic acids				
p-Hydroxybenzoic acid	0.03 ± 0.01	0.03 ± 0.02	0.03 ± 0.01	0.06 ± 0.11
Other compounds				
Lauroside B	0.37 ± 0.35	0.37 ± 0.38	0.29 ± 0.35	0.34 ± 0.27
Azelaic acid	0.45 ± 0.45	0.73 ± 1.07	0.64 ± 1.03	0.49 ± 0.41

and ligstroside over the rest.

Results are expressed as mean ± SD. For each parameter, columns with different letters indicate statistically significant differences between subpopulations ($p < 0.05$). Abbreviations: 1-β-D-Glu-ACD elenolic acid I1: 1-β-D-Glucopyranosyl acyclodihydroelenolic acid isomer 1; 1-β-D-Glu-ACD elenolic acid I2: 1-β-D-Glucopyranosyl acyclodihydroelenolic acid isomer 2; A-DM elenolic acid: aldehydic form of decarboxymethyl elenolic acid; D-OH elenolic acid I2: decarboxylated form of hydroxy elenolic acid isomer 2; EA: elenolic acid; glu: glucoside; H-DA-DM elenolic acid: hydrated product of the dialdehydic form of decarboxymethyl elenolic acid; Hy-DA-DM elenolic acid I1: hydroxylated product of the dialdehydic form of decarboxymethyl elenolic acid isomer 1; Hy-DA-DM elenolic acid I2: hydroxylated product of the dialdehydic form of decarboxymethyl elenolic acid isomer 2; *m/z*: mass to charge ratio; OL: olive leaves; I: isomer; rut: rutinoside.

FRAP seems to be more influenced by flavonoid contents in comparison with COX inhibitory activity. In this case, the 25 % of the flavonoids studied were statistically different between F1 and F4 subpopulations, while about 19 % and 50 % of the flavonoids studied were different in COX-2 and AChE on their specific subpopulations, respectively. Specifically, OL extracts from F1 showed the highest content in luteolin 7-*O*-glucoside over the rest. Similarly, the isorhamnetin 3-*O*-β-D-(6-p-coumaroyl) glucoside, apigenin-7-*O*-glucoside, azelaic acid, and chrysoeriol-7-*O*-glucoside contents were also higher, but only compared with those OL extracts from F4 subgroup. Likewise, luteolin-7-*O*-glucoside, the hydroxycoumarins, hydroxytyrosol, as well as verbascoside contents were also distinguished on F1 over the rest, indicating a possible modulatory effect of these compounds on ferric reducing antioxidant capacity.

3.4. Partial least squares-discriminant analysis and correlation analysis

PLS-DA is a useful algorithm that can be used for predictive and descriptive modelling as well as for discriminative variable selection. PLS-DA has demonstrated great success in modelling high-dimensional datasets for diverse purposes such as metabolomics and food analysis (Lee et al., 2018). In the present study, a value higher than 1 (which correspond to $P < 0.05$), was considered as the selection criterion for the variable of importance in projection (VIP) score of the PLS-DA and was indicated with a discontinued vertical line in Fig. 1B, 2B, and 3B. In the same way, Pearson's correlation analysis was used to corroborate the results obtained in VIP score (Table S4).

Fig. 1A, provides the PLS-DA analysis based on AChE inhibitory activity subpopulations, which showed a different distribution between subgroup 1 and 4 (high *vs.* low AChE inhibitory activity). The PLS-DA analysis revealed an interesting trend in the spatial distribution towards the top-right part of the plot, indicating an increase in AChE

Table 3
Phytochemical profile (milligram of compound per gram of dry weight) of the OL extracts based on FRAP.

	F4	F3	F2	F1
Secoiridoids				
1-β-D-Glu-ACD EA I1	0.33 ± 0.25	0.36 ± 0.22	0.29 ± 0.13	0.25 ± 0.19
1-β-D-Glu-ACD EA I2	0.38 ± 0.40^{a}	0.86 ± 0.53^{b}	0.86 ± 0.63^{b}	0.48 ± 0.55^{ab}
A-DM EA	0.32 ± 0.44	0.20 ± 0.26	0.10 ± 0.12	0.09 ± 0.09
D-OH EA I2	0.08 ± 0.19	–	–	–
H-DA-DM EA	0.05 ± 0.13	0.04 ± 0.13	0.06 ± 0.10	0.03 ± 0.04
Hy-DA-DM EA I1	0.10 ± 0.13	0.13 ± 0.11	0.12 ± 0.11	0.06 ± 0.12
Hy-DA-DM EA I2	0.30 ± 0.56	0.19 ± 0.25	0.21 ± 0.27	0.09 ± 0.17
Hydroxyoleuropein	0.01 ± 0.03^{a}	0.10 ± 0.11^{a}	0.10 ± 0.16^{a}	0.70 ± 0.67^{b}
Ligstroside	–	–	–	0.44 ± 0.44
Oleoside	0.23 ± 0.48^{a}	0.69 ± 1.20^{a}	0.22 ± 0.45^{a}	2.70 ± 2.77^{b}
Oleoside methyl ester	0.27 ± 0.47^{a}	0.50 ± 0.71^{a}	0.26 ± 0.30^{a}	2.00 ± 1.92^{b}
Oleuropein	0.159 ± 0.232^{a}	0.912 ± 0.824^{a}	1.29 ± 2.31^{a}	20.3 ± 22.20^{b}
Oleuropein diglu	–	–	–	0.23 ± 0.29
Oleuropein I	–	0.01 ± 0.02^{a}	0.06 ± 0.20^{a}	2.07 ± 2.25^{b}
Flavonoids				
(+)-Eriodictyol	0.04 ± 0.09	0.12 ± 0.13	0.08 ± 0.10	0.08 ± 0.11
Apigenin	0.18 ± 0.14	0.11 ± 0.08	0.16 ± 0.18	0.26 ± 0.37
Apigenin-7-*O*-glu	0.15 ± 0.15^{a}	0.32 ± 0.20^{ab}	0.25 ± 0.17^{ab}	0.40 ± 0.25^{b}
Apigenin-7-*O*-rut	0.40 ± 0.22^{ab}	0.50 ± 0.21^{b}	0.45 ± 0.24^{b}	0.27 ± 0.17^{a}
Chrysoeriol-7-*O*-glu	0.40 ± 0.30^{a}	0.61 ± 0.18^{b}	0.57 ± 0.22^{ab}	0.61 ± 0.25^{b}
Diosmetin	0.29 ± 0.14	0.19 ± 0.09	0.23 ± 0.12	0.20 ± 0.23
I-3-*O*-β-D-glu	0.01 ± 0.01	0.01 ± 0.02	0.03 ± 0.03	0.06 ± 0.09
Luteolin	0.29 ± 0.17	0.25 ± 0.20	0.38 ± 0.26	0.25 ± 0.15
Luteolin 7-*O*-glu	0.48 ± 0.37^{a}	0.82 ± 0.23^{a}	0.88 ± 0.29^{a}	2.13 ± 1.73^{b}
Luteolin glu	2.66 ± 2.07	4.33 ± 2.35	4.50 ± 2.34	3.85 ± 1.80
Luteolin rut I1	–	–	–	0.01 ± 0.01
Luteolin rut I2	0.01 ± 0.04	0.01 ± 0.02	0.03 ± 0.05	0.03 ± 0.05
Luteolin-7,4-*O*-diglu	0.07 ± 0.08	0.10 ± 0.08	0.10 ± 0.08	0.06 ± 0.07
Oxidized quercetin	–	–	0.01 ± 0.01	–
Taxifolin	–	0.01 ± 0.00	–	0.01 ± 0.02
Phenolic alcohols				
Hydroxytyrosol	0.05 ± 0.04^{a}	0.08 ± 0.05^{a}	0.09 ± 0.06^{a}	0.29 ± 0.15^{b}
Hydroxytyrosol glu	0.16 ± 0.22	0.38 ± 0.53	0.29 ± 0.36	0.59 ± 0.74
4-Ethylguaiacol	0.11 ± 0.10	0.09 ± 0.06	0.10 ± 0.06	0.08 ± 0.04
Iridoids				
Loganic acid	0.18 ± 0.11^{a}	0.27 ± 0.07^{b}	0.22 ± 0.08^{ab}	0.22 ± 0.12^{ab}
7-Epiloganin	0.61 ± 0.37	0.67 ± 0.25	0.61 ± 0.25	0.78 ± 0.29
Lamiol	0.64 ± 0.54	1.00 ± 0.25	0.86 ± 0.45	0.64 ± 0.48
Hydroxycoumarins				
Esculetin	0.06 ± 0.05^{a}	0.11 ± 0.06^{a}	0.15 ± 0.11^{ab}	0.38 ± 0.30^{b}
Esculin	0.02 ± 0.03^{a}	0.06 ± 0.05^{ab}	0.04 ± 0.03^{a}	0.09 ± 0.06^{b}
Hydroxycinnamic acid				
Verbascoside	0.10 ± 0.04^{a}	0.13 ± 0.05^{a}	0.23 ± 0.20^{a}	0.75 ± 0.58^{b}
Decaffeoylverbascoside	1.11 ± 0.95^{ab}	1.52 ± 0.84^{b}	1.35 ± 0.90^{ab}	0.72 ± 0.48^{a}
Phenolic acids				
p-Hydroxybenzoic acid	0.03 ± 0.02	0.03 ± 0.02	0.02 ± 0.02	0.07 ± 0.11
Other compounds				
Lauroside B	0.22 ± 0.25^{a}	0.52 ± 0.39^{b}	0.41 ± 0.34^{ab}	0.24 ± 0.27^{a}
Azelaic acid	0.21 ± 0.12^{a}	0.32 ± 0.31^{a}	0.61 ± 0.79^{ab}	1.13 ± 1.11^{b}

inhibitory activity. In the same way, a bigger phytochemical profile variation within A1 populations than the rest of the groups was also identified. The VIP score for AChE inhibitory activity showed that over 40 % of the studied compounds might exert a modulatory effect on cholinergic function. Among the compounds of interest, over the 35 % corresponded to flavonoids. Luteolin-7-*O*-glucoside content showed the greatest VIP score and Pearson's correlation value in the inhibition of AChE activity exerted by OL extracts (Fig. 1B). This result is in accordance with those *in vitro* studies that reported a remarkably potent inhibitory activity of luteolin-7-*O*-glucoside even at lower doses than those present in the A1 subpopulation (Rehfeldt et al., 2022; Sezen Karaoğlan et al., 2023). Similarly, luteolin and its derivatives and isoharmnentin derivatives also exhibited a moderate AChE inhibitory activity in Ellman *in vitro* assay (Olennikov et al., 2017; Omar et al., 2018). In the same way, apigenin derivatives also showed a potential AChE inhibitory activity according to a molecular docking study (Olajide & Sarker, 2020).

On the other hand, the VIP score shows that over 40 % of the compounds of interest were secoiridoids, suggesting that this family was involved in the cholinergic modulatory activity exerted by OL extracts. Oleuropein and its derivatives were the compounds with more contribution in the A1 subpopulation. Despite the results obtained in VIP score and the moderate association value, *in vitro* studies demonstrated that isolated oleuropein presents a very low AChE inhibitory activity in Ellman test (Omar et al., 2018). However, oleuropein supplementation has shown to improve ACh content in brains from rodent models of cerebral stroke (Gao et al., 2020). This incongruence between *in vitro* and *in vivo* experiments might be explained by the rapid and partial hydrolysis of oleuropein in the upper gastrointestinal tract to hydroxytyrosol and its derivatives (Romero-Márquez, Forbes-Hernández, et al., 2023). Phenolic compounds with multiple hydroxyl groups are believed to enhance the AChE inhibitory activity due to their stronger binding capacity (Jabir et al., 2018). However, the role of hydroxyoleuropein in AChE inhibitory activity has not been explored and there is not data available to compare. Nonetheless, the phenolic alcohol hydroxytyrosol showed a significant VIP score, with demonstrated inhibitory activity of AChE *in vitro* (Costanzo et al., 2021). Other compounds detected by VIP score with null effect in AChE inhibitory activity were loganic acid and verbascoside (Omar et al., 2018; Wang et al., 2021). Nonetheless, the enrichment of OL with individual compounds may increase the inhibitory activity. In this context, an OL extract with a lower oleuropein content than A1 but similar with A2 subgroup exerted a remarkable inhibitory activity of AChE but was 2.7 times lower than OL extract 25 % enriched in hydroxytyrosol (Omar et al., 2018). Similarly, just as the

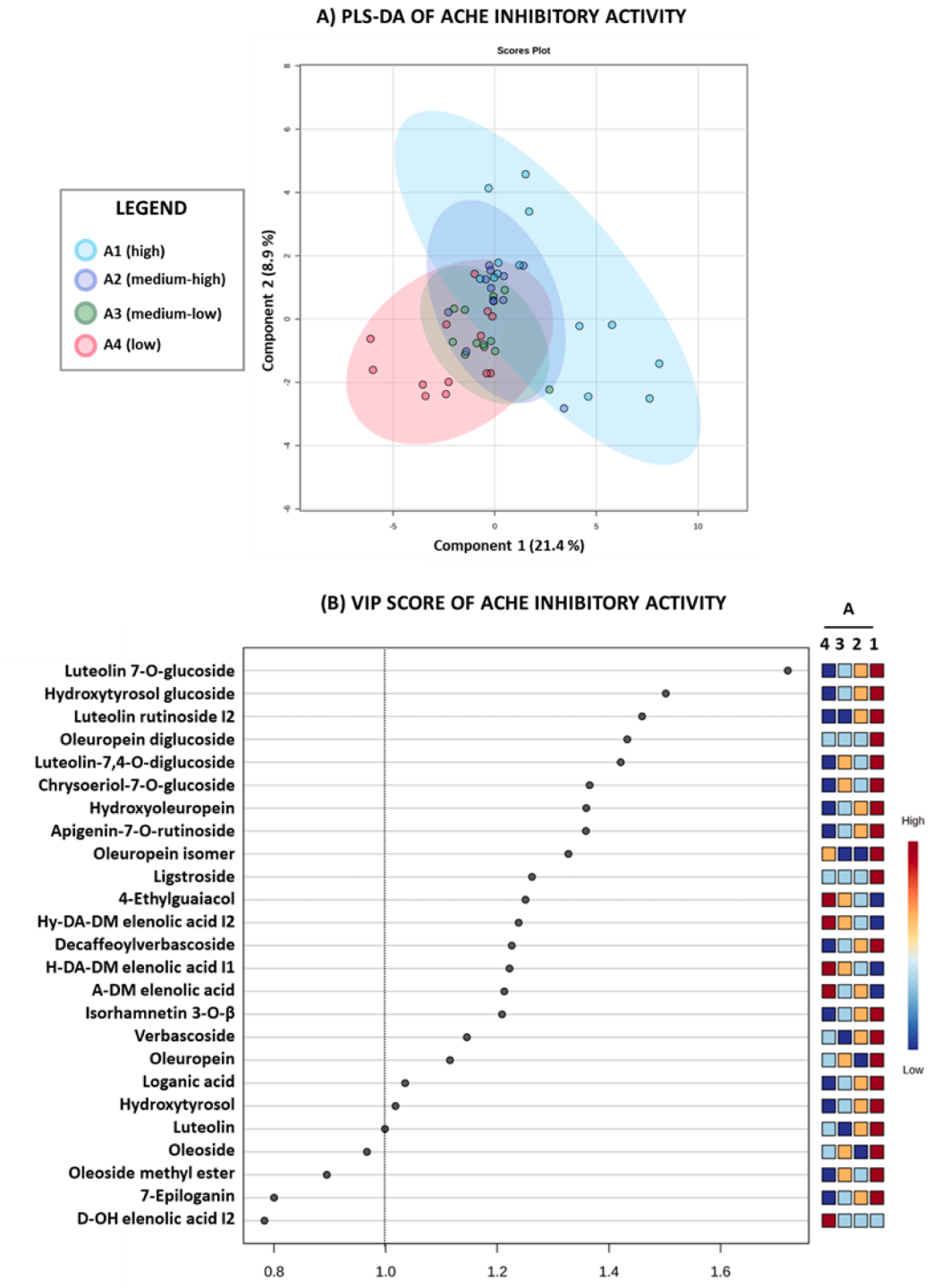

Fig. 1. (A) Partial least squares discriminant analyses (PLS-DA) scores plot obtained from the mean values of the 42 phytochemical compounds present in the OL from the different subpopulations of inhibitory activity of AChE. (B) Variable importance in projection (VIP) score plots for the top 25 most important phytochemical compounds by PLS-DA. The heatmap indicates the relative concentration of the specific compound in the different subpopulations and the dashed line means statistically significant at $p < 0.05$. Abbreviations: A-DM elenolic acid: aldehydic form of decarboxymethyl elenolic acid; D-OH elenolic acid I2: decarboxylated form of hydroxy elenolic acid isomer 2; H-DA-DM elenolic acid: hydrated product of the dialdehydic form of decarboxymethyl elenolic acid; Hy-DA-DM elenolic acid I2: hydroxylated product of the dialdehydic form of decarboxymethyl elenolic acid isomer 2; I: isomer.

enrichment of certain compounds may enhance the inhibitory activity, evidence indicates that some compounds might diminish the AChE inhibitory activity of olive leaves. In the present research, A4 subgroup presented the highest elenolic acid derivatives content over the rest. The VIP score for these compounds oscillate between 1.2 and 1.4, indicating a potential role of these compounds in the AChE inhibitory activity. Pearsons's correlation analysis demonstrated a moderate and negative association among these compounds and the AChE inhibitory activity of OL extracts (Table S4). This inverse association has been previously reported in OL samples from Greece, which exhibited a very low AChE inhibitory activity and were strongly and negatively correlated with the content of the elenolic acid derivatives (Romero-Márquez, Forbes-Hernández, et al., 2023). This feature was also observed in a study evaluating the AChE inhibitory activity of different varieties of extra-

virgin olive oil (Figueiredo-González et al., 2018). These results might be explained due to the fact that these compounds, are linked to oleuropein, hydroxytyrosol, and ligstroside structures, and an excess of these free elenolic acid derivatives might indicate an excessive degradation of oleuropein, hydroxytyrosol, and ligstroside, which may reduce the AChE inhibitory properties of OL extracts (Granados-Principal et al., 2010).

Concerning COX-2 inhibitory activity, the PLS-DA analysis showed that the distribution of the different subpopulations seems to follow the same trend as AChE inhibitory activity tests but is less obvious between subgroup 1 and 4 (high *vs.* low COX-2 inhibitory activity), probably due to the smaller therapeutic range exerted by OL samples in comparison with AChE inhibitory activity (Fig. 2A). In the present PLS-DA analysis, no discernible differences in spatial distribution were observed between groups 2, 3 and 4, indicating similarities among them. The VIP score for COX-2 inhibitory activity showed that almost 30 % of the studied compounds might exert a modulatory effect on inflammatory function. Among the compounds of interest, less of the 20 % corresponded to

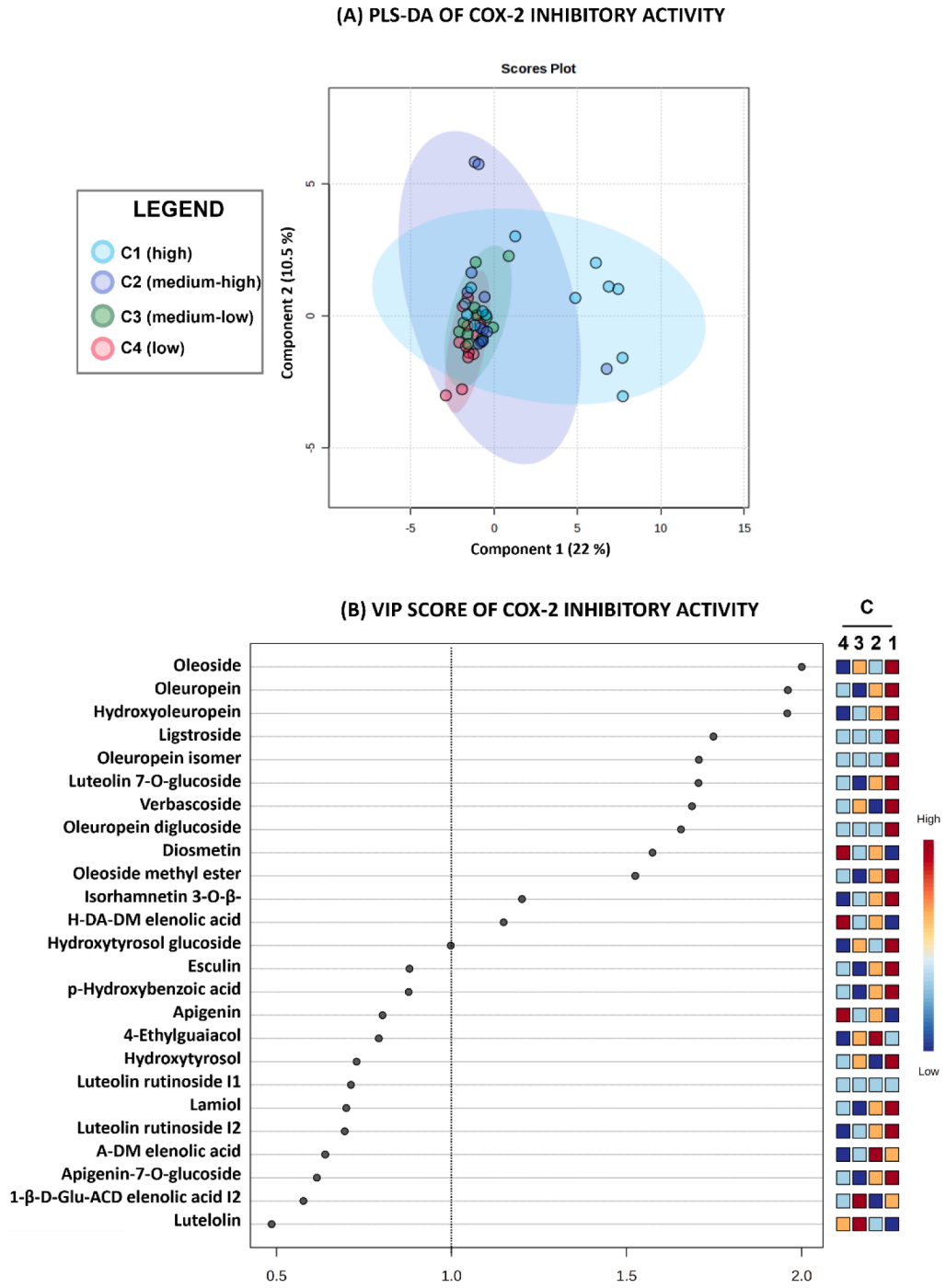

Fig. 2. (A) Partial least squares discriminant analyses (PLS-DA) scores plot obtained from the mean values of the 42 phytochemical compounds present in the OL from the different subpopulations of inhibitory activity of COX-2. (B) Variable importance in projection (VIP) score plots for the top 25 most important phytochemical compounds by PLS-DA. The heatmap indicates the relative concentration of the specific compound in the different subpopulations and the dashed line means statistically significant at $p < 0.05$. Abbreviations: 1-β-D-Glu-ACD elenolic acid I1: 1-β-D-Glucopyranosyl acyclodihydroelenolic acid isomer 1; A-DM elenolic acid: aldehydic form of decarboxymethyl elenolic acid; H-DA-DM elenolic acid: hydrated product of the dialdehydic form of decarboxymethyl elenolic acid; I: isomer.

flavonoids (Fig. 2B). Luteolin-7-*O*-glucoside content had the greatest VIP score and Pearson's correlation value in the flavonoid family regarding to COX-2 inhibitory activity. This result is in accordance with a study reporting a remarkably potent COX-2 inhibitory activity of luteolin-7-*O*-glucoside in an hepatitis-induced ICR mice (Park & Song, 2019). Similarly, Isorhamnetin 3-*O*-β-D-(6-p-coumaroyl) glucoside also exhibited a moderate positive correlation, but the research about the inhibitory COX-2 activity is null. In contrast, diosmetin was more abundant in the OL extracts from C4 subpopulations and exhibited a negative association with COX-2 inhibitory activity (Table S4). From a biosynthetic point of view, flavonoids are derived from a limited number of flavanone intermediates. The production of diosmetin can occur through two enzymatic pathways: via the enzyme flavone *O*-methyltransferase using luteolin as a substrate, or by the enzyme flavanone 3′-hydroxylase using apigenin as a substrate (Grignon-Dubois & Rezzonico, 2012). Luteolin is a substrate necessary to the formation of luteolin-7-*O*-glucoside, a

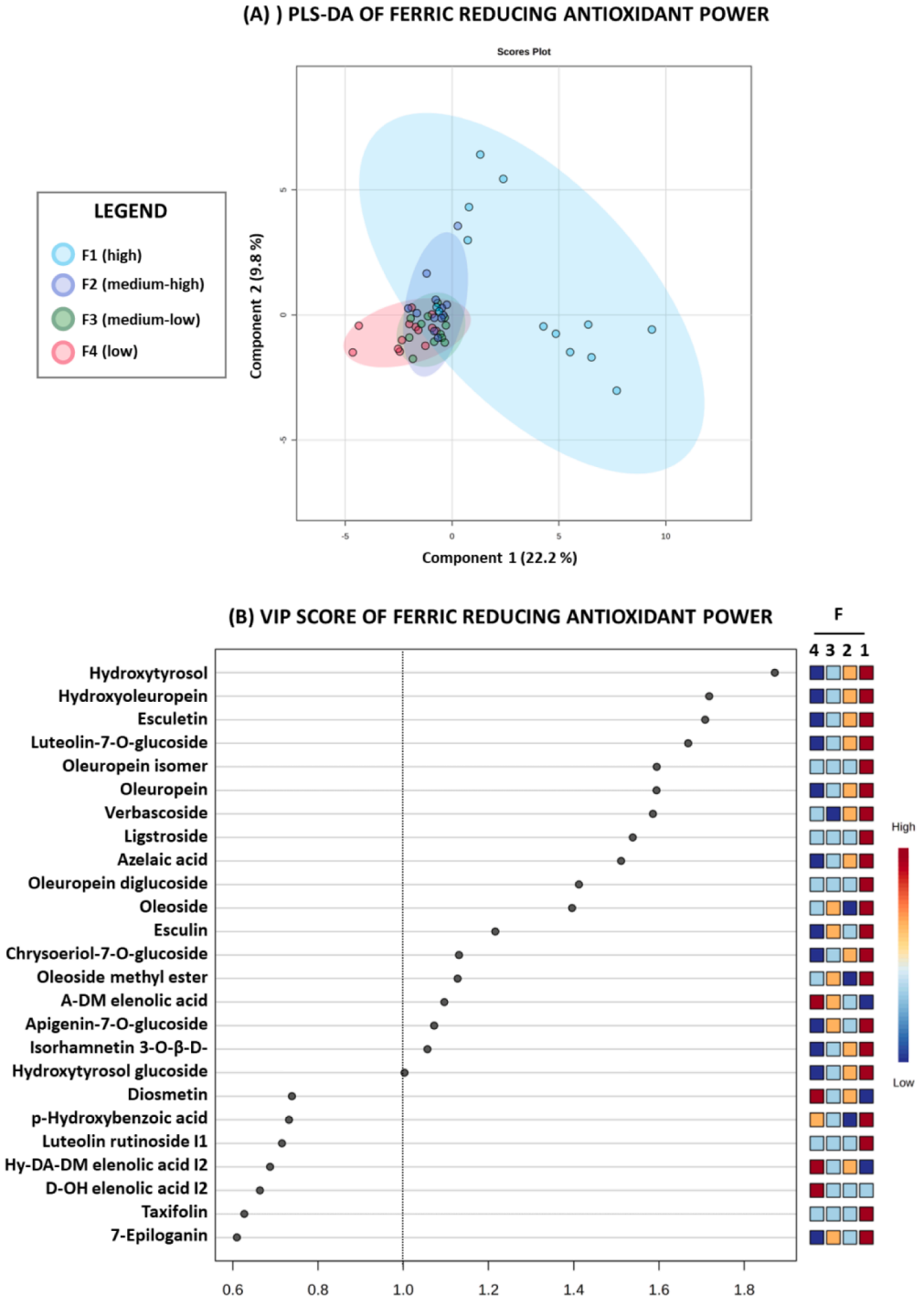

Fig. 3. (A) Partial least squares discriminant analyses (PLS-DA) scores plot obtained from the mean values of the 42 phytochemical compounds present in the OL from the different subpopulations of inhibitory activity of FRAP. (B) Variable importance in projection (VIP) score plots for the top 25 most important phytochemical compounds by PLS-DA. The heatmap indicates the relative concentration of the specific compound in the different subpopulations and the dashed line means statistically significant at $p < 0.05$. Abbreviations: A-DM elenolic acid: aldehydic form of decarboxymethyl elenolic acid; D-OH elenolic acid I2: decarboxylated form of hydroxy elenolic acid isomer 2; Hy-DA-DM elenolic acid I2: hydroxylated product of the dialdehydic form of decarboxymethyl elenolic acid isomer 2; I: isomer.

flavonoid with a remarkable anti-inflammatory effect. Therefore, the formation of diosmetin might compromise the formation of luteolin-7-*O*-glucoside. Consequently, this process might potentially lead to a reduction in the COX-2 inhibitory activity due to a reduction in luteolin-7-*O*-glucoside.

On the other hand, the VIP score showed that 50 % of the compounds of interest were secoiridoids, indicating that this family was strongly involved in the anti-inflammatory activity exerted by OL extracts. In this context, oleoside content had the greatest VIP score and one of the higher Pearson's correlation values in the secoiridoids family regarding to COX-2 inhibitory activity (Fig. 2B). However, there is no evidence of the modulatory effect of this compound or its derivatives on COX-2 activity, but it opens the field for further research to test the anti-inflammatory capacity of oleoside. Despite the limitation, PLS-DA assigned to oleuropein and its derivatives a significantly high VIP score and these findings were further supported by Pearson's correlation analysis (Table S4). The anti-inflammatory activity of these compound is well described. For instance, oleuropein consumption has been related to COX-2 protein levels reduction under pro-inflammatory conditions such as ulcerative colitis in humans (Larussa et al., 2017). Other secoiridoid detected by VIP score with high positive correlation values were ligstroside and the aldehydic form of decarboxymethyl elenolic acid (A-DM elenolic acid). It has been demonstrated by molecular docking that verbascoside selectively inhibits COX (Liang et al., 2020), whereas the role of A-DM elenolic acid has not yet been explored. In the present research, A4 subgroup had the highest hydroxylated product of the dialdehydic form of decarboxymethyl elenolic acid isomer 2 content and was negatively correlated with COX-2 inhibitory activity (Table S4) in a similar way as previously proposed for the AChE inhibitory activity. Among hydroxycinnamic acids studied, verbascoside was pointed out by PLS-DA and Pearson's analysis. In that sense, C1 subpopulation presented the highest verbascoside content (Table 2). In fact, verbascoside has shown to reduce the expression of COX-2 *in vitro* (Pesce et al., 2015).

Finally, regarding the ferric reducing antioxidant capacity, the PLS-DA analysis revealed a distinct distribution between groups 1 and 4 (high *vs.* low FRAP) as shown in Fig. 3A. There was a clear overlap in spatial distribution of the subpopulation F2 and F3, while group 1 exhibited a significant differentiation, probably attributed to its remarkable antioxidant capacity. The VIP score for FRAP showed that among 40 % of the studied compounds might exert a modulatory effect on antioxidant capacity. In this context, hydroxytyrosol received the greatest VIP score and Pearsons's correlation value over the rest. The antioxidant property of hydroxytyrosol and its derivatives, has been widely described using FRAP test *in vitro* (Romero-Márquez, Navarro-Hortal, Jiménez-Trigo, Muñoz-Ollero, et al., 2022). In addition, hydroxytyrosol supplementation has been shown to increase the ferric reducing antioxidant capacity of plasma in a mouse model of systemic inflammation (Fuccelli et al., 2018).

On the other hand, the VIP score showed that 35 % of the compounds of interest were secoiridoids, suggesting that this family was strongly involved in the antioxidant activity exerted by OL extracts (Fig. 3B). In this context, oleuropein, and its derivatives received one of the higher VIP score and Pearson's correlation values. F1 subpopulation had the highest content in oleuropein and its derivatives over the rest. *In vitro* studies demonstrated that the FRAP of OL increases with the content of oleuropein (Ghasemi et al., 2018; Martín-García et al., 2022). PLS-DA assigned significantly high VIP score to oleoside and its derivatives as well as ligstroside content, and these findings were further supported by Pearson's correlation analysis (Table S4). These results agrees with those obtained in different *in vitro* studies, which demonstrated that the ferric reducing antioxidant capacity of OL increases with the content of oleoside and ligstroside (Martín-García et al., 2022). In contrast, the secoiridoid A-DM elenolic acid was negatively correlated with FRAP (Table S4). This association could be explained similarly to the proposition in the AChE inhibitory activity section (Granados-Principal et al., 2010).

Among the compounds of interest, less than 25 % corresponded to flavonoids (Fig. 3B). Luteolin-7-*O*-glucoside contents had the greatest VIP score and Pearson's correlation within the flavonoid family about antioxidant activity. This result is in accordance with a study that reported a remarkably potent ferric reducing antioxidant capacity of luteolin-7-*O*-glucoside which was able to reduce DNA oxidative markers in RAW264.7 cells (Rehfeldt et al., 2022). PLS-DA assigned apigenin-7-*O*-glucoside a significantly high VIP score and these findings were further supported by a study that demonstrated that the FRAP of OL increases with the content of apigenin-7-*O*-glucoside (Martín-García et al., 2022).

Other compounds pointed out by VIP score and corroborated with Pearsons's correlation analysis were hydroxycoumarins (esculetin and esculin), verbascoside as well as azelaic acid content. These compounds were mainly present in F1 subpopulation, indicating a strong contribution to the antioxidant activity exerted by OL. These results are consistent with those reported in the literature, as esculetin, esculin, and verbascoside have been identified as potent ferric reducing antioxidant agents (Leal et al., 2023; Martín-García et al., 2022). Similarly, azelaic acid also exhibited a moderate positive correlation, with promising results against paraquat-induced oxidative stress in *C. elegans* (Bai et al., 2021). This work underlines the continued significance of bioactive compounds across various fields, aligning with prior research findings (Abd-Ella et al., 2022; Liu et al., 2021; Y. Zhang et al., 2023).

4. Conclusions

This study provides a comprehensive characterization of the phytochemical profile of fifty olive leaf extracts and evaluates the role of its phytochemical composition in the anti-inflammatory, anti-cholinergic, and antioxidant activities. The investigation into individual compounds reveals that flavonoids, particularly luteolin-7-*O*-glucoside, isoharmnentin, and apigenin derivatives, significantly contribute to anti-cholinesterase activity. Secoiridoids, such as oleuropein and ligstroside, play a crucial role in COX-2 inhibitory activity, while diosmetin appears to be negatively associated. Both secoiridoids and flavonoids contribute equally to the observed antioxidant effect, with specific compounds like oleuropein, ligstroside, luteolin-7-*O*-glucoside, hydroxytyrosol, hydroxycoumarins, and verbascoside playing key roles in the ferric reducing antioxidant capacity.

The project's merit lies in providing valuable insights into the nuanced roles of individual phytochemicals within olive leaf extracts. On the other hand, a limitation of this study is the use of *in vitro* tests, which do not account for biological interactions and the complexity of physiological systems. Additionally, while multivariate analysis can identify important variables for sample selection, it does not establish causal associations. Nevertheless, the application of both VIP scores and Pearson's correlation allows for the confirmation that the specific phytochemical compound is highlighted in various tests, enabling the assignment of a role in the observed effect. Taken together, this research provides valuable insights and confirms the initial hypothesis that specific compounds within OL extracts contribute to distinct anti-cholinergic, anti-inflammatory, and anti-oxidative effects. Moving forward, the project's future scope involves expanding investigations to incorporate *in vivo* models, thereby advancing our understanding and potential therapeutic applications of olive leaf extracts.

Funding

This research was funded by the SUSTAINOLIVE research grant, funded by the PRI-MA EU program, and by the grant PID2019-106778RB-I00, funded by MCIN/AEI/https://doi.org/10.13039/501100011033 FEDER "Una manera de hacer Europa".

CRediT authorship contribution statement

Jose M. Romero-Márquez: Writing – review & editing, Writing – original draft, Methodology, Investigation, Formal analysis. **María D. Navarro-Hortal:** Methodology, Formal analysis. **Tamara Y. Forbes-Hernández:** Writing – review & editing, Visualization, Resources, Methodology, Investigation, Conceptualization. **Alfonso Varela-López:** Methodology, Investigation. **Juan G. Puentes:** Methodology, Investigation, Formal analysis. **Cristina Sánchez-González:** Resources, Funding acquisition, Conceptualization. **Sandra Sumalla-Cano:** Visualization, Resources, Funding acquisition. **Maurizio Battino:** Resources, Investigation, Funding acquisition, Conceptualization. **Roberto García-Ruiz:** Investigation, Funding acquisition, Conceptualization. **Sebastián Sánchez:** Supervision, Resources, Funding acquisition, Conceptualization. **José L. Quiles:** .

Declaration of competing interest

The authors declare that they have no known competing financial interests or personal relationships that could have appeared to influence the work reported in this paper.

Data availability

Data will be made available on request.

Acknowledgments

José M. Romero-Márquez is a FPU fellow with grant reference FPU2018/05301, funded by MCIN/AEI/10.13039/501100011033 and FSE "El FSE invierte en tu futuro". Tamara Forbes-Hernández is supported by a JdC-I postdoctoral contract with grant reference IJC2020-043910-I, funded by NextGenerationEU. María D. Navarro-Hortal is supported by "Contratos-Puente" funded by Universidad de Granada.

Appendix A. Supplementary data

Supplementary data to this article can be found online at https://doi.org/10.1016/j.foodchem.2024.138516.

References

Abd-Ella, A., Metwally, S., ul-Malik, M., El-Ossaily, Y., Elrazek, F., Aref, S., Naffea, Y., & Abdel-Raheem, S. (2022). A review on recent advances for the synthesis of bioactive pyrazolinone and pyrazolidinedione derivatives. *Current Chemistry Letters, 11*(2), 157–172.

Alcántara, C., Žugčić, T., Abdelkebir, R., García-Pérez, J. V., Jambrak, A. R., Lorenzo, J. M., Collado, M. C., Granato, D., & Barba, F. J. (2020). Effects of Ultrasound-Assisted Extraction and Solvent on the Phenolic Profile, Bacterial Growth, and Anti-Inflammatory/Antioxidant Activities of Mediterranean Olive and Fig Leaves Extracts. *Molecules, 25*(7). https://doi.org/10.3390/molecules25071718

Bai, J., Farias-Pereira, R., Jang, M., Zhang, Y., Lee, S. M., Kim, Y.-S., Park, Y., Ahn, J. B., Kim, G.-H., & Kim, K.-H. (2021). Azelaic Acid Promotes Caenorhabditiselegans Longevity at Low Temperature Via an Increase in Fatty AcidDesaturation. *Pharmaceutical Research, 38*(1), 15–26. https://doi.org/10.1007/s11095-020-02975-w

Blazakis, K. N., Kosma, M., Kostelenos, G., Baldoni, L., Bufacchi, M., & Kalaitzis, P. (2017). Description of olive morphological parameters by using open access software. *Plant Methods, 13*, 111. https://doi.org/10.1186/s13007-017-0261-8

Costanzo, P., Oliverio, M., Maiuolo, J., Bonacci, S., De Luca, G., Masullo, M., Arcone, R., & Procopio, A. (2021). Novel Hydroxytyrosol-Donepezil Hybrids as Potential Antioxidant and Neuroprotective Agents. *Frontiers Chemistry, 9*. https://www.frontiersin.org/articles/10.3389/fchem.2021.741444.

Ellman, G. L., Courtney, K. D., Andres, V., & Feather-Stone, R. M. (1961). A new and rapid colorimetric determination of acetylcholinesterase activity. *Biochemical Pharmacology, 7*, 88–95. https://doi.org/10.1016/0006-2952(61)90145-9

Espeso, J., Isaza, A., Lee, J. Y., Sörensen, P. M., Jurado, P., Avena-Bustillos, R.de. J., Olaizola, M., & Arboleya, J. C. (2021). Olive Leaf Waste Management. *Frontiers in Sustainable Food Systems., 5*, P0. https://www.frontiersin.org/articles/10.3389/fsufs.2021.660582.

Figueiredo-González, M., Reboredo-Rodríguez, P., González-Barreiro, C., Carrasco-Pancorbo, A., Simal-Gándara, J., & Cancho-Grande, B. (2018). Nutraceutical Potential of Phenolics from 'Brava' and 'Mansa' Extra-Virgin Olive Oils on the Inhibition of Enzymes Associated to Neurodegenerative Disorders in Comparison with Those of 'Picual' and 'Cornicabra'. *Molecules, 23*(4), Article 4. https://doi.org/10.3390/molecules23040722

Fuccelli, R., Fabiani, R., & Rosignoli, P. (2018). Hydroxytyrosol Exerts Anti-Inflammatory and Anti-Oxidant Activities in a Mouse Model of Systemic Inflammation. *Molecules (Basel, Switzerland), 23*(12), 3212. https://doi.org/10.3390/molecules23123212

Gao, Y., Li, X., Xu, R., Guo, Y., Yin, H., Tan, R., Qi, Z., Liu, G., Liang, J., & Ya, B. (2020). Oleuropein Improved Post Cerebral Stroke Cognitive Function by Promoting Histone Acetylation and Phosphorylation of cAMP Response Element-Binding Protein in MCAO Rats. *Dose-Response: A Publication of International Hormesis Society, 18*(3). https://doi.org/10.1177/1559325820950102

Ghasemi, S., Koohi, D. E., Emmamzadehhashemi, M. S. B., Khamas, S. S., Moazen, M., Hashemi, A. K., Amin, G., Golfakhrabadi, F., Yousefi, Z., & Yousefbeyk, F. (2018). Investigation of phenolic compounds and antioxidant activity of leaves extracts from seventeen cultivars of Iranian olive (Olea europaea L.). *Journal of Food Science and Technology, 55*(11), 4600–4607. https://doi.org/10.1007/s13197-018-3398-1

Granados-Principal, S., Quiles, J. L., Ramirez-Tortosa, C. L., Sanchez-Rovira, P., & Ramirez-Tortosa, M. C. (2010). Hydroxytyrosol: From laboratory investigations to future clinical trials. *Nutrition Reviews, 68*(4), 191–206. https://doi.org/10.1111/j.1753-4887.2010.00278.x

Grignon-Dubois, M., & Rezzonico, B. (2012). First Phytochemical Evidence of Chemotypes for the Seagrass Zostera noltii. *Plants, 1*(1). https://doi.org/10.3390/plants1010027

Jabir, N. R., Khan, F. R., & Tabrez, S. (2018). Cholinesterase targeting by polyphenols: A therapeutic approach for the treatment of Alzheimer's disease. *CNS Neuroscience & Therapeutics, 24*(9), 753–762. https://doi.org/10.1111/cns.12971

Lama-Muñoz, A., Contreras, M.del. M., Espínola, F., Moya, M., Romero, I., & Castro, E. (2020). Content of phenolic compounds and mannitol in olive leaves extracts from six Spanish cultivars: Extraction with the Soxhlet method and pressurized liquids. *Food Chemistry, 320*, Article 126626. https://doi.org/10.1016/j.foodchem.2020.126626

Larussa, T., Oliverio, M., Suraci, E., Greco, M., Placida, R., Gervasi, S., Marasco, R., Imeneo, M., Paolino, D., Tucci, L., Gulletta, E., Fresta, M., Procopio, A., & Luzza, F. (2017). Oleuropein Decreases Cyclooxygenase-2 and Interleukin-17 Expression and Attenuates Inflammatory Damage in Colonic Samples from Ulcerative Colitis Patients. *Nutrients, 9*(4), 391. https://doi.org/10.3390/nu9040391

Leal, L. E., Moreira, E. S., Correia, B. L., Bueno, P. S. A., Comar, J. F., de Sá-Nakanishi, A. B., Cuman, R. K. N., Bracht, A., Bersani-Amado, C. A., & Bracht, L. (2023). Comparative study of the antioxidant and anti-inflammatory effects of the natural coumarins 1,2-benzopyrone, umbelliferone and esculetin: In silico, in vitro and in vivo analyses. *Naunyn-Schmiedeberg's Archives of Pharmacology*. https://doi.org/10.1007/s00210-023-02606-2

Lee, L. C., Liong, C.-Y., & Jemain, A. A. (2018). Partial least squares-discriminant analysis (PLS-DA) for classification of high-dimensional (HD) data: A review of contemporary practice strategies and knowledge gaps. *The Analyst, 143*(15), 3526–3539. https://doi.org/10.1039/C8AN00599K

Liang, J., Bonvino, N. P., Hung, A., & Karagiannis, T. C. (2020). In silico characterisation of olive phenolic compounds as potential cyclooxygenase modulators. Part 1. *Journal of Molecular Graphics & Modelling, 101*, Article 107719. https://doi.org/10.1016/j.jmgm.2020.107719

Liu, L., Zhang, Y., Tang, L., Zhong, H., Danzeng, D., Liang, C., & Liu, S. (2021). The Neuroprotective Effect of *Byu d Mar* 25 in LPS-Induced Alzheimer's Disease Mice Model. *Evidence-Based Complementary and Alternative Medicine, 2021*, e8879014.

Martín-García, B., De Montijo-Prieto, S., Jiménez-Valera, M., Carrasco-Pancorbo, A., Ruiz-Bravo, A., Verardo, V., & Gómez-Caravaca, A. M. (2022). Comparative Extraction of Phenolic Compounds from Olive Leaves Using a Sonotrode and an Ultrasonic Bath and the Evaluation of Both Antioxidant and Antimicrobial Activity. *Antioxidants (Basel, Switzerland), 11*(3), 558. https://doi.org/10.3390/antiox11030558

Olajide, O. A., & Sarker, S. D. (2020). Alzheimer's disease: Natural products as inhibitors of neuroinflammation. *Inflammopharmacology, 28*(6), 1439–1455. https://doi.org/10.1007/s10787-020-00751-1

Olennikov, D. N., Kashchenko, N. I., Chirikova, N. K., Akobirshoeva, A., Zilfikarov, I. N., & Vennos, C. (2017). Isorhamnetin and Quercetin Derivatives as Anti-Acetylcholinesterase Principles of Marigold (Calendula officinalis) Flowers and Preparations. *International Journal of Molecular Sciences, 18*(8), 1685. https://doi.org/10.3390/ijms18081685

Omar, S. H., Scott, C. J., Hamlin, A. S., & Obied, H. K. (2018). Biophenols: Enzymes (β-secretase, Cholinesterases, histone deacetylase and tyrosinase) inhibitors from olive (Olea europaea L.). *Fitoterapia, 128*, 118–129. https://doi.org/10.1016/j.fitote.2018.05.011

Park, C. M., & Song, Y.-S. (2019). Luteolin and luteolin-7-O-glucoside protect against acute liver injury through regulation of inflammatory mediators and antioxidative enzymes in GalN/LPS-induced hepatitic ICR mice. *Nutrition Research and Practice, 13*(6), 473–479. https://doi.org/10.4162/nrp.2019.13.6.473

Pesce, M., Franceschelli, S., Ferrone, A., De Lutiis, M. A., Patruno, A., Grilli, A., Felaco, M., & Speranza, L. (2015). Verbascoside down-regulates some pro-inflammatory signal transduction pathways by increasing the activity of tyrosine phosphatase SHP-1 in the U937 cell line. *Journal of Cellular and Molecular Medicine, 19*(7), 1548–1556. https://doi.org/10.1111/jcmm.12524

Rehfeldt, S. C. H., Silva, J., Alves, C., Pinteus, S., Pedrosa, R., Laufer, S., & Goettert, M. I. (2022). Neuroprotective Effect of Luteolin-7-O-Glucoside against 6-OHDA-Induced Damage in Undifferentiated and RA-Differentiated SH-SY5Y Cells. *International Journal of Molecular Sciences, 23*(6), 2914. https://doi.org/10.3390/ijms23062914

Rivas-García, L., Quiles, J. L., Roma-Rodrigues, C., Raposo, L. R., Navarro-Hortal, M. D., Romero-Márquez, J. M., Esteban-Muñoz, A., Varela-López, A., García, L. C., Cianciosi, D., Forbes Hernández, T. Y., Battino, M., Llopis, J., Fernandes, A. R., Baptista, P. V., & Sánchez-González, C. (2021). Rosa x hybrida extracts with dual actions: Antiproliferative effects against tumour cells and inhibitor of Alzheimer disease. *Food and Chemical Toxicology, 149*, Article 112018. https://doi.org/10.1016/j.fct.2021.112018

Rivas-García, L., Romero-Márquez, J. M., Navarro-Hortal, M. D., Esteban-Muñoz, A., Giampieri, F., Sumalla-Cano, S., Battino, M., Quiles, J. L., Llopis, J., & Sánchez-González, C. (2022). Unravelling potential biomedical applications of the edible flower Tulbaghia violacea. *Food Chemistry, 381*, Article 132096. https://doi.org/10.1016/j.foodchem.2022.132096

Romero-Márquez, J. M., Forbes-Hernández, T. Y., Navarro-Hortal, M. D., Quirantes-Piné, R., Grosso, G., Giampieri, F., Lipari, V., Sánchez-González, C., Battino, M., & Quiles, J. L. (2023). Molecular Mechanisms of the Protective Effects of Olive Leaf Polyphenols against Alzheimer's Disease. *International Journal of Molecular Sciences, 24*(5), 4353. https://doi.org/10.3390/ijms24054353

Romero-Márquez, J. M., Navarro-Hortal, M. D., Forbes-Hernández, T. Y., Varela-López, A., Puentes, J. G., Pino-García, R. D., Sánchez-González, C., Elio, I., Battino, M., García, R., Sánchez, S., & Quiles, J. L. (2023). Exploring the Antioxidant, Neuroprotective, and Anti-Inflammatory Potential of Olive Leaf Extracts from Spain, Portugal, Greece, and Italy. *Antioxidants, 12*(8). https://doi.org/10.3390/antiox12081538

Romero-Márquez, J. M., Navarro-Hortal, M. D., Jiménez-Trigo, V., Muñoz-Ollero, P., Forbes-Hernández, T. Y., Esteban-Muñoz, A., Giampieri, F., Delgado Noya, I., Bullón, P., Vera-Ramírez, L., Battino, M., Sánchez-González, C., & Quiles, J. L. (2022). An Olive-Derived Extract 20% Rich in Hydroxytyrosol Prevents β-Amyloid Aggregation and Oxidative Stress, Two Features of Alzheimer Disease, via SKN-1/NRF2 and HSP-16.2 in Caenorhabditis elegans. *Antioxidants, 11*(4), 629. https://doi.org/10.3390/antiox11040629

Romero-Márquez, J. M., Navarro-Hortal, M. D., Jiménez-Trigo, V., Vera-Ramírez, L., Forbes-Hernández, T. J., Esteban-Muñoz, A., Giampieri, F., Bullón, P., Battino, M., Sánchez-González, C., & Quiles, J. L. (2022). An oleuropein rich-olive (Olea europaea L.) leaf extract reduces β-amyloid and tau proteotoxicity through regulation of oxidative- and heat shock-stress responses in Caenorhabditis elegans. *Food and Chemical Toxicology: An International Journal Published for the British Industrial Biological Research Association, 162*, Article 112914. https://doi.org/10.1016/j.fct.2022.112914

Romero-Márquez, J. M., Varela-López, A., Navarro-Hortal, M. D., Badillo-Carrasco, A., Forbes-Hernández, T. Y., Giampieri, F., Domínguez, I., Madrigal, L., Battino, M., & Quiles, J. L. (2021). Molecular Interactions between Dietary Lipids and Bone Tissue during Aging. *International Journal of Molecular Sciences, 22*(12), 6473. https://doi.org/10.3390/ijms22126473

Sezen Karaoğlan, E., Hancı, H., Koca, M., & Kazaz, C. (2023). Some Bioactivities of Isolated Apigenin-7-O-glucoside and Luteolin-7-O-glucoside. *Applied Sciences, 13*(3). https://doi.org/10.3390/app13031503

Wang, Z. Y., Zhang, X. D., & Whang, W. K. (2021). The Effect of Terpenoids of Dipsacus Asperoides Against Alzheimer's Disease and Development of Simultaneous Analysis by High Performance Liquid Chromatography. *Natural Product Communications, 16*(9). https://doi.org/10.1177/1934578X211044603

Zhang, C., Xin, X., Zhang, J., Zhu, S., Niu, E., Zhou, Z., & Liu, D. (2022). Comparative Evaluation of the Phytochemical Profiles and Antioxidant Potentials of Olive Leaves from 32 Cultivars Grown in China. *Molecules (Basel, Switzerland), 27*(4), 1292. https://doi.org/10.3390/molecules27041292

Zhang, Y., Zeng, M., Li, B., Zhang, B., Cao, B., Wu, Y., Ye, S., Xu, R., Zheng, X., & Feng, W. (2023). Ephedra Herb extract ameliorates adriamycin-induced nephrotic syndrome in rats via the CAMKK2/AMPK/mTOR signaling pathway. *Chinese Journal of Natural Medicines, 21*(5), 371–382. https://doi.org/10.1016/S1875-5364(23)60454-6